



Published in final edited form as:

Biochemistry. 2011 April 5; 50(13): 2541–2549. doi:10.1021/bi101906y.

## Identification of StARD3 as a Lutein-binding Protein in the Macula of the Primate Retina<sup>†</sup>

Binxing Li, Preejith Vachali, Jeanne M. Frederick, and Paul S. Bernstein\*

Department of Ophthalmology and Visual Sciences, Moran Eye Center, University of Utah School of Medicine, Salt Lake City, UT 84132

### Abstract

Lutein, zeaxanthin and their metabolites are the xanthophyll carotenoids that form the macular pigment of the human retina. Epidemiological evidence suggests that high levels of these carotenoids in the diet, serum and macula are associated with decreased risk of age-related macular degeneration (AMD), and the AREDS2 study is prospectively testing this hypothesis. Understanding the biochemical mechanisms underlying the selective uptakes of lutein and zeaxanthin into the human macula may provide important insights into the physiology of the human macula in health and disease. GSTP1 is the macular zeaxanthin-binding protein, but the identity of the human macular lutein-binding protein has remained elusive. Prior identification of the silkworm lutein-binding protein (CBP) as a member of the steroidogenic acute regulatory domain (StARD) protein family, and selective labeling of monkey photoreceptor inner segments by anti-CBP antibody provided an important clue toward identifying the primate retina lutein-binding protein. Homology of CBP to all 15 human StARD proteins was analyzed using database searches, western blotting and immunohistochemistry, and we here provide evidence to identify StARD3 (also known as MLN64) as a human retinal lutein-binding protein. Further, recombinant StARD3 selectively binds lutein with high affinity ( $K_D = 0.45$  micromolar) when assessed by surface plasmon resonance (SPR) binding assays. Our results demonstrate previously unrecognized, specific interactions of StARD3 with lutein and provide novel avenues to explore its roles in human macular physiology and disease.

While more than 600 carotenoids are known to exist in nature, only lutein, zeaxanthin and their metabolites are present in the human retina (1-4). These two xanthophyll carotenoids are concentrated spatially in the foveal region of the *macula lutea*, forming the “yellow spot” of macular pigment described by 18<sup>th</sup> century anatomists (5). Lutein and zeaxanthin participate in maintaining the health and function of the human macula through their light screening and antioxidant properties (1). Epidemiological studies have linked high levels and dietary intakes of lutein and zeaxanthin with decreased risk of age-related macular degeneration (AMD) (6-9), and currently, the AREDS2 study is evaluating the efficacy of daily supplementation of 10 mg of lutein and 2 mg of zeaxanthin in a randomized, placebo-controlled manner among high risk AMD patients.

Primates do not possess enzymes known to synthesize or interconvert the various carotenoids, although the ocular conversion of lutein to *meso*-zeaxanthin and various simple xanthophyll redox reactions are likely to be enzymatically mediated. Thus, all macular lutein

<sup>†</sup>This work is supported by National Institute of Health Grant EY-11600, by Kemin Health (Des Moines, Iowa, USA), and by Research to Prevent Blindness, Inc. (New York, NY).

\*Corresponding author: Paul S. Bernstein, MD, PhD, Moran Eye Center, 65 Mario Capecchi Drive, University of Utah, Salt Lake City, UT 84132, U. S. A., Tel.: 801-581-6078, Fax: 801-581-3357, paul.bernstein@hsc.utah.edu.

and zeaxanthin are considered to be derived from either supplements or a typical American diet of 1-2 mg of lutein and ~0.2 mg of zeaxanthin per day, primarily from dark green leafy vegetables and orange and yellow fruits and vegetables (7,9). Of the 30-50 carotenoids in the human diet, only about 15 are detectable in the serum (10). Similar diversity is present in the pigmented structures of the eye such as the ciliary body, iris and retinal pigment epithelium (RPE), while the retina exclusively is enriched in lutein and zeaxanthin (11). Within the retina there is further specificity. In the fovea, the carotenoid concentration approaches 1 mM, and the ratio of lutein to zeaxanthin to *meso*-zeaxanthin (a metabolite of lutein) is 1:1:1 (12). The concentration of macular carotenoids declines over 100-fold just a few millimeters from the foveal center, and the composition ratio approaches 3:1:0 in the peripheral retina (11).

Among mammals, the specific uptake of lutein and zeaxanthin to millimolar concentrations into macular retina appears to be unique to humans and fellow primates. In invertebrates, such specificity is ordinarily driven by high-affinity binding proteins such as crustacyanin, an astaxanthin-binding protein in lobster shells (13), but until recently no such carotenoid-binding proteins had been identified in any vertebrates beyond relatively low-affinity and low-specificity bloodstream transport proteins, e.g., albumin and various lipoproteins. Our laboratory reported that GSTP1 is the zeaxanthin-binding protein of the human macula (14), and in 2009, we partially purified a lutein-binding protein from human retina (15). The protein preparation, which was highly enriched with endogenous lutein, cross-reacted with an antibody raised against the silkworm gut lutein-binding protein (CBP) on western blots, and the same antibody specifically labeled photoreceptor inner segments and axons in monkey macula sections (15). This suggested that the human retinal lutein-binding protein is likely to be a member of the steroidogenic acute regulatory domain (StARD) protein family, just as CBP. Here, we provide evidence further identifying StARD3 (a protein also known as MLN64) as a human macular lutein-binding protein.

## EXPERIMENTAL PROCEDURES

### Western blots

Human donor eyes were procured through the Utah Lions Eye Bank in compliance with tenets of the Declaration of Helsinki. Dissection of the globes was performed within 24 hours postmortem on ice and under dim light. Macula and peripheral retina punches were excised with a circular trephine (8-mm diameter), and vitreous was removed by pipette during the dissection. Underlying retinal pigment epithelium (RPE)/choroid were then isolated. Mouse retina and RPE/choroid were harvested under dim light. Human and mouse tissues were washed twice with PBS and homogenized in 10 mM Tris-HCl buffer (pH7.4) containing 0.2 mM PMSF and 10 µg/mL aprotinin to prepare total protein extracts.

Proteins were separated on 4–15% gradient SDS–PAGE and transferred to 0.45 µm nitrocellulose membranes using a trans-blot SD semi-dry transfer cell (Bio-Rad, Hercules, CA) at 20 V for 1 h. Nonspecific binding was blocked by immersing the membrane in 5% (w/v) nonfat dried milk in 0.01% (v/v) Tween 20 in TBS for 1 h at room temperature on an orbital shaker. The membranes were rinsed briefly with two changes of TBS and incubated with primary antibody overnight. Primary antibodies to StARD1 (mouse monoclonal antibody, H00006770-M01), StARD2 (mouse polyclonal antibody, H00058488-B01), StARD4 (mouse polyclonal antibody, H00134429-B01), StARD5 (mouse polyclonal antibody, H00080765-B01), StARD11 (rabbit polyclonal antibody, NB100-2113), StARD12 (goat polyclonal antibody, NB300-917), and StARD14 (mouse monoclonal antibody, H00026027-M01) were from Novus Biological, Inc. (Littleton, CO). Primary antibodies to StARD6–StARD10 (goat polyclonal antibodies, sc-67853, sc-67855, sc-67859, sc-67863, sc-54336, respectively) and StARD13 (goat polyclonal antibody, sc67843) were from Santa

Cruz Biotechnology, Inc. (Santa Cruz, CA). Primary antibody to StARD3 (rabbit polyclonal antibody, N-62 StAR) was a gift from Professor Walter L. Miller at UCSF (San Francisco, CA). Primary antibody to StARD15 (rabbit polyclonal antibody, ARP52535-P050) was from Aviva System Biology (San Diego, CA). Anti-StARD3 primary antibody was diluted 1:5000, and the dilution ratios of the other fourteen StARD antibodies were 1:500-1000. The antibody to actin (1:500 dilution) came from Sigma-Aldrich (St. Louis, MO). Activity of the antibodies was confirmed with the relevant proteins or peptides.

After two changes of wash buffer, the membranes were incubated with horseradish peroxidase-conjugated secondary antibody (1:1000 polyclonal donkey anti-goat IgG-HRP, rabbit anti-mouse IgG-HRP, or goat anti-rabbit IgG (H+L)-HRP) for 2 h at room temperature. To visualize bands, membranes were developed using ECL Plus Western blot detection reagents (Amersham Biosciences, Pittsburgh, PA).

### Reverse Transcription-Polymerase Chain Reaction

Total RNA (2 $\mu$ g) was prepared from human retina. cDNA was synthesized using SuperScript™ II Reverse transcriptase (Invitrogen, Carlsbad, CA). PCR amplification was performed using 1 $\mu$ l reaction as template. GAPDH primers were: forward 5'-GCTGGCGCTGAGTACGTCG -3' and reverse 5'-TGCCAGCCCCAGCGTCAAAG-3', yielding a 635 bp amplicon. StARD3 primers were: forward 5'-GGGACAGTTCTATTACCCCCAG-3' and reverse 5'-TGTCGCAGGTGAAAGGCAAATTCAAAC-3', giving an amplicon of 728 bp. PCR conditions were: denaturation at 94°C for 5 min; 35 cycles of 94°C for 30 s, annealing at 55°C for 30 s, and extension at 72°C for 30 s, with final extension for 7 min. Products were evaluated by electrophoresis on an ethidium bromide-stained 1% agarose gel in 1 $\times$  TBE buffer. The related products were individually cloned and sequenced.

### Immunohistochemistry

Confocal microscope images derive from a 6-7 year old male *Macaca mulatta* monkey whose eyes were perfused with 4% paraformaldehyde in 0.1 M phosphate buffer for 15 minutes (time of day 1900). After removal of each anterior segment and vitreous, the eyecups were rinsed and cryoprotected overnight in 0.1 M phosphate buffer (pH 7.4, 4°C) containing 15% sucrose. The eyecups were transferred to 0.1 M phosphate buffer containing 30% sucrose the next morning and held for 8 hours at 4°C. For each eyecup, a macular punch centered approximately on the fovea was isolated, embedded and frozen at -70°C. Cryosections 12  $\mu$ m-thick were cut, rinsed in 0.1 M phosphate buffer containing 0.1% Triton X-100 (PBT) and blocked for 1 h using 10% normal donkey serum in PBT. Antibodies to StARD3 (N-62, 1:5000 dilution) and cone arrestin (7G6 from Peter R. MacLeish; Morehouse School of Medicine, Atlanta, GA; characterized by Zhang, *et al.* (16) and used at 1:2000 dilution) or glutamine synthetase (BD Bioscience, 1:1000 dilution) were applied overnight at 4°C. After rinsing in PBT (10 minutes  $\times$  3) rhodamine- and FITC-conjugated secondary antibodies (Jackson ImmunoResearch Laboratories, West Grove, PA; Cat. #711-295-152 and 715-096-150, each 1:200 dilution) were co-applied for 2 h at room temperature. Immunolocalization was imaged using a Zeiss LSM 510 confocal microscope set to an optical slice of <0.9  $\mu$ m. Control sections, in which incubation in primary antibodies was omitted, were processed in parallel and found to be negative for retina immunoreactivity.

### Surface plasmon resonance (SPR) binding studies

Amine coupling reagents N-hydroxysuccinimide, 1-ethyl-3-(3-dimethylaminopropyl)-carbodiimide hydrochloride, GST coupling kit, and 1 M sodium ethanolamine hydrochloride (pH 8.5) were used according to recommendations of the manufacturer (Biacore AB,

Uppsala, Sweden). Fatty-acid-free human serum albumin (HSA) (Sigma-Aldrich, St. Louis, MO), GSTP1 (Oxford Biomedical Research, USA), and StARD3-GST fusion protein (Novus Biologicals, Littleton, CO) were used as supplied. Recombinant carotenoid binding protein from silkworm *Bombyx mori* (CBP), cloned into an expression plasmid (from Professor Kozo Tsuchida, National Institute of Infectious Diseases, Shinjuku, Tokyo, Japan), was expressed and purified as described (17). Gifts of carotenoids include: (3R, 3'R)-zeaxanthin (ZeaVision, St. Louis, MO), (3R, 3'S-*meso*)-zeaxanthin (DSM, Basel, Switzerland), (3R, 3'R, 6'R)-lutein (Kemin Health, Des Moines, IA) and (3S, 3'S)-astaxanthin (Cardax Pharmaceutical, Aiea, HI). All carotenoids were crystalline, with >98% isomeric and chemical purity confirmed by HPLC.

HSA, GSTP1, and CBP (50 µg/mL in 10 mM sodium acetate, pH 4.5-5) were each immobilized on individual sensor chip surfaces using a standard amine-coupling protocol (flow rate of 10 µl/min). GST-tagged StARD3 was immobilized using a GST-antibody coupling protocol to obtain a density of 10-12 kRU. Each of the five carotenoids was dissolved in 0.4 mM sucrose monolaurate (Mitsubishi Chemicals, Japan) to achieve high concentration, and 10 mM PBS (pH 7.4) with 0.01% Triton X-100 and 0.4 mM sucrose monolaurate was used as the running buffer. Carotenoid concentration series were prepared as two-fold dilutions into running buffer. Typically, the carotenoid concentration series spanned 0.01–10 µM. Multiple blanks were included in each analysis. Five blanks were analyzed at the beginning, and remaining blanks were interspersed throughout for double-referencing purposes. Protein binding of all carotenoids was performed at a flow rate of 30 µl/min, with monitoring of association and dissociation for 2 and 10 minutes, respectively. For cholesterol analysis, 3-hexanoyl-NBD cholesterol (Cayman Chemicals, Cayman, MI) was dissolved in 100% DMSO and diluted in PBS (10 mM PBS, 0.01% Triton X-100, pH 7.4) to a final DMSO concentration of 5%.

Surface plasmon resonance measurements were recorded on a SensiQ (ICx Nomadics; Oklahoma City, OK) instrument at a controlled temperature of 25°C. SensiQ employs a miniature SPR-based sensor. The sensor is designed in a Kretschmann's configuration, whereby monochromatic light is reflected from the sensing surface over a range of incident angles, and the reflectance minimum will occur with respect to the incident angle and is detected by a photodiode array. The sensing surface is a planar glass chip with ~50 nm gold film coating.

Affinity determination SPR response data (sensorgrams) were zeroed on both the response and time axes at the beginning of each injection and double referenced. First, bulk refractive index changes were corrected by subtracting the responses generated over an unmodified reference surface from the binding responses generated over the protein surfaces. Second, any systematic artifacts observed between the proteins and reference flow cells were corrected by subtracting the response generated by an average of the buffer injections from the binding responses generated by carotenoid injections. Simple interactions were adequately fit to a steady-state, single-site, bimolecular interaction model ( $A+B=AB$ ) yielding a single  $K_D$  for HSA, CBP, GSTP1 and StARD3.

### Lutein-StARD3 pigment-protein complex detection by absorption spectrum

StARD3 protein binding domain (residues 216-444) was expressed in BL21 (DE3) cells (Invitrogen, Carlsbad, CA) using an expression vector, pET22b-His-StARTdomain (a gift from Professor James H. Hurley, NIH (Bethesda, MD)) (18). After purification using His-Select Nickel Affinity Gel (Sigma-Aldrich, St. Louis, MO), 100 µg StARD3 binding domain protein was incubated overnight with lutein (two-fold excess) in a buffer containing 50 mM PBS, pH 8.0, and 8 mM CHAPS at 4°C. This incubated solution was loaded on a silica gel filtration column (BIOSEP-SEC-S 3000 PEEK; 300 × 7.80 mm; separation range, 5-700

kDa; Phenomenex, Torrance, CA), and 50 mM sodium phosphate buffer (pH 7.0) containing 8 mM CHAPS was used as the eluant at a 0.3 ml/min flow rate. Protein chromatography was performed on a BioLogic liquid chromatography system (Bio-Rad, Hercules, CA), and the eluates were monitored by a UV6000LP photodiode array spectrophotometer (Thermo Scientific, Waltham, MA). Unbound carotenoid was then eluted from the column with methanol.

## RESULTS

### Comparison of silkworm CBP to human StARD proteins

We reported previously that an antibody to the silkworm lutein-binding protein known as CBP can specifically label lutein-binding protein purified from human retina and the layers of the primate macula where the macular carotenoid pigment is at its highest concentration (15). Silkworm CBP shares significant homology and cross-reactivity with human StARD proteins which participate in the transfer processes of hydrophobic molecules, such as cholesterol and lipids (17,19). Therefore, there is a high possibility that the retinal lutein-binding protein is a member of the StARD family. We first compared the amino acid sequence of CBP to all 15 human StARD proteins. Figure 1 shows that all human StARD proteins share some homology with CBP, especially in the binding domain, but StARD1 and StARD3 exhibit the most homology, followed by StARD4 and StARD5 and then StARD6. These results are in accord with the initial description of silkworm CBP in which it was reported that CBP and StARD3 (also known as MLN64) share 29% sequence homology (17).

### Expression of StARD proteins in human and mouse retina and RPE/choroid

Knowledge of expression of StARD proteins in human retina is very limited. We therefore used a series of antibodies directed against all 15 human and mouse StARD proteins for qualitative western blotting against mouse and human tissue extracts normalized against actin (Table1). Only StARD3 and StARD8 were detected in human retina, and they were not found in mouse retina. StARD3 and StARD8 were also detectable in human and mouse RPE/choroid. StARD6 was present in mouse retina and RPE/choroid but not in human ocular tissues. Human and mouse liver had very different StARD protein expression patterns relative to ocular tissues.

StARD3 exhibited the pattern most consistent with a potential lutein-binding protein with a single band more strongly expressed in the macula relative to the peripheral retina on western blots normalized to actin (Figure 2A). Human retinal mRNA expression of StARD3 was also confirmed by RT-PCR (Figure 2B). Although StARD8 protein is also expressed in human retina, its protein expression is not macula-enhanced (Table 1), and its protein sequence has among the lowest homologies of all members of the human StARD family relative to silkworm CBP (Figure 1). Therefore, all subsequent studies described here focused on determining whether StARD3 is a physiologically relevant lutein-binding protein in the human macula.

### Immunohistochemistry of StARD3 in primate macula

Highest quality immunohistochemistry is often performed on monkey rather human ocular tissue because human and monkey retinas share common anatomy, their proteins are highly homologous (98% sequence identity in the case of StARD3), and perfusion fixation can be performed immediately at the time of death, minimizing postmortem artifacts. The well characterized polyclonal antibody N-62 StAR (a gift from Professor Walter L. Miller) recognizes the binding domains of both StARD1 and StARD3 in humans (20,21), and we confirmed that it also reacts identically when incubated with monkey retinal extracts;

however, since there is no StARD1 in human (and presumably monkey) retina (see Table 1, also confirmed by RT-PCR), all immunostaining can be considered to originate from StARD3 immunoreactivity as long proper pre-absorption controls are performed (see below). Immunoreactivity attributable to StARD3 was contrasted with that of primate cone arrestin (Figures 3-4) or glutamine synthetase (Figure 5) in cryosections cut from monkey retina/RPE/choroid isolated using a trephine (8-mm diameter) centered on the fovea and passing through a portion of the optic nerve. Transverse sections were cut parallel to the plane formed by a line from the fovea to optic nerve.

Figure 3 (top panel) shows a low-magnification view of cone arrestin labeling near the foveal pit. Arrestins comprise a gene family participating in the regulation of G protein-coupled receptors and their signaling cascades (22,23). Visual arrestins, rod (arrestin-1) and cone (arrestin-4), distribute according to light history. In light, cone arrestin accumulates most intensely in the outer segment to quench opsin signaling while in dark, the soluble protein translocates to the inner segment (16). Absent direct observation of macular carotenoid pigment in sections, arrestin (mAb 7G6) labeling served to identify cones and verify the near-foveal location owing to high packing density and axons of Henle's fiber layer (Figure 3, lower panels, green). By contrast, StARD3 (pAb N-62) labeling was found distributed broadly across the retinal expanse, in all nuclear layers, and prominently in Henle's fiber layer (Figure 3, lower panels, red).

Within the photoreceptor layer of the monkey parafovea, N-62 StAR labeling was present in both rods and cones. Cone inner segments were labeled preferentially, as were their axons forming the Henle fiber layer and synaptic pedicles (red signal of Figure 4 A, B). Thus, regions of high cone density were observed to be relatively enriched for StARD3, consistent with the known distribution of the macular carotenoid pigment in primate retina (2, 12, 24-26). To determine antibody specificity for StARD3 protein, N-62 StAR primary antibody was pre-absorbed with StARD3 recombinant protein prior to overnight incubation with a foveal section. Relative to an adjacent, positive control section that was exposed to N-62 StAR antibody of the same dilution and incubated/imaged under identical conditions (Figure 4C), preabsorption by StARD3 recombinant protein resulted in disappearance of > 90% retina immunofluorescence (Figure 4D), confirming that N-62 StAR antibody labeled StARD3 in monkey retina specifically. Labeling intensity dropped dramatically in the retina periphery. Signal over the RPE is apparently nonspecific, appearing in the absence of primary antibody and despite preabsorption with recombinant protein.

While StARD3 labeling was found in all nuclear layers (outer nuclear layer, inner nuclear layer and ganglion cell layer) of macular retina, it did not co-localize with labeling for glutamine synthetase, a glial cell marker (Figure 5 A,B). Müller cell glia, stretching from the external limiting membrane to the vitreal surface (internal limiting membrane), have extensions that wrap intimately around neuronal processes. With the resolution afforded by a confocal microscope, axons in cross-section were observed to be labeled for StARD3 but not for glutamine synthetase. Conversely, Müller cell endfeet at the vitreal surface were immunoreactive with antibody directed against glutamine synthetase, but not for StARD3 (Figure 5C).

### **Binding affinities of StARD3 relative to other carotenoid-binding proteins**

We immobilized a series of proteins known to associate with carotenoids to compare their binding affinities and specificities to StARD3 using surface plasmon resonance (SPR). Figure 6A shows the SDS-PAGE of human full-length StARD3-GST fusion protein (from Novus Biologicals). StARD3 antibody can strongly label this human recombinant protein with an appropriate apparent molecular weight of ~80 kDa (Figure 6B).

Each recombinant or purified protein was immobilized onto gold surfaces, and then the indicated carotenoids solubilized with 0.4 mM sucrose monolaurate were passed over the chip in stepped concentrations in a microcapillary. Equilibrium dissociation constants ( $K_D$ ) were calculated using one-site and multiple-site models with appropriate correction for nonspecific binding using a second channel reference chip without immobilized protein. As shown in Table 2, the high affinity binding site on GSTP1, the previously reported retinal zeaxanthin-binding protein, had the highest affinity  $K_D$  ( $\sim 0.10 \mu\text{M}$ ) when zeaxanthin and *meso*-zeaxanthin were the presented ligands, while the other three carotenoid showed much lower binding affinities. A second, lower affinity carotenoid binding site was also detectable on GSTP1 for the zeaxanthins and astaxanthin when solubilized at higher concentrations in 5% dimethylsulfoxide (DMSO), but  $K_D$  values were generally  $\sim 5 \mu\text{M}$ . Silkworm CBP and human StARD3 were similarly specific for lutein with  $K_D$  values of  $0.18 \mu\text{M}$  and  $0.45 \mu\text{M}$ , respectively. Representative sensorgrams and binding curves of lutein and zeaxanthin interactions with StARD3 are shown in Figure 7. On the other hand, human serum albumin (HSA) exhibited minimal preference among the various carotenoids tested, and all  $K_D$  values were  $>1 \mu\text{M}$ . Since it has been reported that StARD3 can also bind cholesterol, we performed SPR experiments as described above using the cholesterol analog 3-hexanoyl-NBD cholesterol dissolved in 5% DMSO. Our observed  $K_D$  value of  $0.12 \mu\text{M}$  corresponds closely to the value reported for interaction of this analog with StARD3 measured by a fluorescence quenching assay (27).

### Absorption spectrum of lutein bound to StARD3

Monomeric binding of carotenoids to proteins usually results in a bathochromic shift of the visible absorption spectrum. We therefore examined whether a similar shift occurs when lutein binds a soluble form of StARD3. The binding domain of StARD3 protein consists of  $\sim 200$  amino acids which form a predominantly hydrophobic tunnel (18,19). Figure 8 (insert) shows the SDS-PAGE of the purified StARD3 binding domain expressed in *E. coli*. After incubating StARD3 binding domain with an excess of lutein ligand, we chromatographically purified the ligand-protein complex. Lutein bound to StARD3 binding domain exhibited a 10 nm shift of its triple peak vibronic structure relative to lutein dissolved in methanol (Figure 8), confirming that StARD3 can bind lutein. This 10 nm bathochromic shift is much smaller than the shift we reported previously for the partially purified lutein-binding protein from human retina (15), but it is quite comparable to the shift that is observed when zeaxanthin is bound to GSTP1 (14).

## DISCUSSION

Steroidogenic acute regulatory domain protein 3 (StARD3) manifests several properties expected of a lutein-binding protein. Shown macula-enriched by immunoblot analysis, StARD3 binds lutein selectively with high-affinity, possesses a spectral shift of lutein's absorption spectrum corresponding well with the *in vivo* macular pigment spectrum, and reveals an immunolocalization overlapping with our previously measured resonance Raman distribution of macular pigment carotenoids (15). Thus StARD3 and GSTP1 proteins provide abundant lutein- and zeaxanthin-binding sites, respectively, that account for the unique distribution and stability of carotenoids found in the primate *macula lutea*.

StARD proteins are known to bind a variety of small hydrophobic ligands. The human StARD family consists of 15 different soluble and membrane-associated proteins that share a common binding domain structure (reviewed by Alpy and Tomasetto, 2005) (19). Cholesterol and phosphatidylcholine are among the best known ligands of StARD proteins, but many more remain to be defined. It was not until the identification of silkworm CBP as the lutein-binding protein in the gut and the silk gland and recognition of CBP as a StARD family member that attention was turned to the potential physiological interactions of

carotenoids and StARD proteins. Using an anti-CBP antibody, positive immunoreactivity was observed against partially purified lutein-binding protein isolated from human retina on immunoblots and on monkey macular tissue sections (15). We undertook a systematic study of multiple commercial and proprietary antibodies raised against all 15 human StARD proteins, and it soon became clear that StARD3 was the likely lutein-binding protein which we subsequently confirmed by SPR binding analysis.

StARD3 function beyond its role as a lutein-binding site in the macula remains to be defined. Some StARD proteins act as intracellular shuttles for their ligands (28,29). It is also possible that StARD3 may enhance antioxidant activity of its carotenoid ligand, just as the GSTP1-zeaxanthin complex (30), or that it may possess enzymatic activity related to further metabolism of ocular carotenoids. Whether lutein and cholesterol compete for the same binding site remains to be determined.

Regulation of StARD3 expression and its relationship to macular pigment levels in health and disease must be explored further. Some human subjects receiving lutein supplementation are “non-responders” who show no change in macular pigment levels despite dramatic rises of serum carotenoids (31), suggesting that their ocular binding sites are already saturated. Others show slow, steady rises in macular pigment that may even continue after cessation of supplementation (8), suggesting that there can be up-regulation of carotenoid-binding proteins in some situations. With age and development of AMD and a rarer earlier-onset maculopathy known as MacTel, macular pigment levels have been shown to decline in many studies in spite of steady serum carotenoid levels (32-34), implying that binding protein levels may play an important underlying role in risk of visual loss from AMD and MacTel. Correlation of coding and non-coding variants of StARD3 and GSTP1 and their macular expression levels with risk of AMD and MacTel could be investigated, but this is likely to be a complex interaction that will need to take into account dietary carotenoid intake and/or serum carotenoid levels as well.

While we cannot exclude the possibility that proteins besides StARD3 may also act as physiologically-relevant lutein binding sites in the primate macula, the finding that organisms as widely divergent as silkworms and humans have employed similar biochemical strategies using StARD family proteins to achieve tissue-specific uptake of lutein is fascinating and suggests further avenues for exploration. Other StARD proteins such as StARD1 may play comparable carotenoid-binding roles in other tissues. Tissue-specific uptake of lutein in silkworm requires not only CBP, but also a CD36-like transmembrane transport protein (35). In human RPE culture, a CD36 relative, scavenger receptor class B, member 1 (SCARB1), appears to be involved in uptake of xanthophyll carotenoids carried by HDL (36,37). While SCARB1 itself does not have good correlation with lutein distribution in immunohistochemistry of primate retina, CD36 is a potential candidate for a surface receptor and transport protein that could interact with StARD3 to mediate high-affinity uptake of carotenoids into the macula (38).

In summary, with the identification of StARD3 as a lutein-binding protein in primate *macula lutea*, we are now developing a more complete biochemical understanding of a fundamental property of this anatomical feature that is unique to the primate retina. Along with GSTP1, expression of these two proteins appears to be up-regulated to facilitate the high levels and extraordinary stability of the macular carotenoid pigment. Further knowledge of the biochemistry and physiology of StARD3 and GSTP1, and identification of additional carotenoid binding, transport, and metabolic proteins should provide key insights into the role of the macular carotenoids in human ocular health and disease, and therapeutic manipulation of these binding proteins' levels could potentially prove to be a useful intervention against degenerative disorders of the human macula.



## Acknowledgments

The authors thank the Utah Lions Eye Bank for providing human donor eyes. We thank Drs. Walter L. Miller, Koza Tsuchida and James H. Hurley for providing helpful antibodies and expression vectors.

## References

1. Krinsky NI, Landrum JT, Bone RA. Biologic mechanisms of the protective role of lutein and zeaxanthin in the eye. *Annu Rev Nutr.* 2003; 23:171–201. [PubMed: 12626691]
2. Landrum JT, Bone RA. Lutein, zeaxanthin, and the macular pigment. *Arch Biochem Biophys.* 2001; 385:28–40. [PubMed: 11361022]
3. Zhao DY, Wintch SW, Ermakov IV, Gellermann W, Bernstein PS. Resonance Raman measurement of macular carotenoids in retinal, choroidal, and macular dystrophies. *Arch Ophthalmol.* 2003; 121:967–972. [PubMed: 12860799]
4. Khachik, F.; Askin, FB.; Lai, K. Distribution, bioavailability, and metabolism of carotenoids in humans. In: Bidlack, Wayne R.; Omaye, Stanley T.; Meskin, Mark S.; Janher, D., editors. *Phytochemical A new paradigm.* CRC press LCC; 1998. p. 76-131.
5. Home E. An account of the orifice in the retina of the human eye, discovered by Professor Soemmering: to which are added proofs of this appearance being extended to the eyes of other animals. *Philos Trans R Soc Lond.* 1798; 2:332–345.
6. Eye Disease Case-Control Study Group. *Arch Ophthalmol.* Vol. 111. 1993. Antioxidant status and neovascular age-related macular degeneration; p. 104-109.
7. Seddon JM, Ajani UA, Sperduto RD, Hiller R, Blair N, Burton TC, Farber MD, Gragoudas ES, Haller J, Miller DT. Dietary carotenoids, vitamins A, C, and E, and advanced age-related macular degeneration. *JAMA.* 1994; 272:1413–1420. [PubMed: 7933422]
8. Landrum JT, Bone RA, Joa H, Kilburn MD, Moore LL, Sprague KE. A one year study of the macular pigment: the effect of 140 days of a lutein supplement. *Exp Eye Res.* 1997; 65:57–62. [PubMed: 9237865]
9. Mares-Perlman JA, Brady WE, Klein R, Klein BE, Bowen P, Stacewicz-Sapuntzakis M, Palta M. Serum antioxidants and age-related macular degeneration in a population-based case-control study. *Arch Ophthalmol.* 1995; 113:1518–1523. [PubMed: 7487619]
10. Khachik F, Spangler CJ, Smith JC Jr, Canfield LM, Pfander H, Steck A. Identification, quantification, and relative concentrations of carotenoids and their metabolites in human milk and serum. *Anal Chem.* 1997; 69:1873–1881. [PubMed: 9164160]
11. Khachik F, de Moura FF, Zhao DY, Aebischer CP, Bernstein PS. Transformations of selected carotenoids in plasma, liver, and ocular tissues of humans and in nonprimate animal models. *Invest Ophthalmol Visual Sci.* 2002; 43:3383–3392. [PubMed: 12407147]
12. Bone RA, Landrum JT, Friedes LM, Gomez CM, Kilburn MD, Menendez E, Vidal I, Wang W. Distribution of lutein and zeaxanthin stereoisomers in the human retina. *Exp Eye Res.* 1997; 64:211–218. [PubMed: 9176055]
13. Wald G, Nathanson N, Jencks WP, Tarr E. Crustacyanin, the blue carotenoid-protein of the lobster shell. *Biol Bull.* 1948; 95:249–250. [PubMed: 18933429]
14. Bhosale P, Larson AJ, Frederick JM, Southwick K, Thulin CD, Bernstein PS. Identification and characterization of a Pi isoform of glutathione S-transferase (GSTP1) as a zeaxanthin-binding protein in the macula of the human eye. *J Biol Chem.* 2004; 279:49447–49454. [PubMed: 15355982]
15. Bhosale P, Li B, Sharifzadeh M, Gellermann W, Frederick JM, Tsuchida K, Bernstein PS. Purification and partial characterization of a lutein-binding protein from human retina. *Biochemistry.* 2009; 48:4798–4807. [PubMed: 19402606]
16. Zhang H, Cuenca N, Ivanova T, Church-Kopish J, Frederick JM, MacLeish PR, Baehr W. Identification and light-dependent translocation of a cone-specific antigen, cone arrestin, recognized by monoclonal antibody 7G6. *Invest Ophthalmol Visual Sci.* 2003; 44:2858–2867. [PubMed: 12824223]

17. Tabunoki H, Sugiyama H, Tanaka Y, Fujii H, Banno Y, Jouni ZE, Kobayashi M, Sato R, Maekawa H, Tsuchida K. Isolation, characterization, and cDNA sequence of a carotenoid binding protein from the silk gland of *Bombyx mori* larvae. *J Biol Chem.* 2002; 277:32133–32140. [PubMed: 12052833]
18. Tsujishita Y, Hurley JH. Structure and lipid transport mechanism of a StAR-related domain. *Nat Struct Biol.* 2000; 7:408–414. [PubMed: 10802740]
19. Alpy F, Tomasetto C. Give lipids a START: the StAR-related lipid transfer (START) domain in mammals. *J Cell Sci.* 2005; 118:2791–2801. [PubMed: 15976441]
20. Bose HS, Whittal RM, Baldwin MA, Miller WL. The active form of the steroidogenic acute regulatory protein, StAR, appears to be a molten globule. *Proc Natl Acad Sci U S A.* 1999; 96:7250–7255. [PubMed: 10377400]
21. Bose HS, Whittal RM, Huang MC, Baldwin MA, Miller WL. N-218 MLN64, a protein with StAR-like steroidogenic activity, is folded and cleaved similarly to StAR. *Biochemistry.* 2000; 39:11722–11731. [PubMed: 10995240]
22. Gurevich EV, Gurevich VV. Arrestins: ubiquitous regulators of cellular signaling pathways. *Genome Biol.* 2006; 7:236. [PubMed: 17020596]
23. Nikonov SS, Brown BM, Davis JA, Zuniga FI, Bragin A, Pugh EN Jr, Craft CM. Mouse cones require an arrestin for normal inactivation of phototransduction. *Neuron.* 2008; 59:462–474. [PubMed: 18701071]
24. Snodderly DM, Auran JD, Delori FC. The macular pigment. II. Spatial distribution in primate retinas. *Invest Ophthalmol Visual Sci.* 1984; 25:674–685. [PubMed: 6724837]
25. Bone RA, Landrum JT. Macular pigment in Henle fiber membranes: a model for Haidinger's brushes. *Vision Res.* 1984; 24:103–108. [PubMed: 6546825]
26. Rapp LM, Maple SS, Choi JH. Lutein and zeaxanthin concentrations in rod outer segment membranes from perifoveal and peripheral human retina. *Invest Ophthalmol Visual Sci.* 2000; 41:1200–1209. [PubMed: 10752961]
27. Reitz J, Gehrig-Burger K, Strauss JF 3rd, Gimpl G. Cholesterol interaction with the related steroidogenic acute regulatory lipid-transfer (START) domains of StAR (STARD1) and MLN64 (STARD3). *FEBS J.* 2008; 275:1790–1802. [PubMed: 18331352]
28. Clark BJ, Stocco DM. Expression of the steroidogenic acute regulatory (StAR) protein: a novel LH-induced mitochondrial protein required for the acute regulation of steroidogenesis in mouse Leydig tumor cells. *Endocr Res.* 1995; 21:243–257. [PubMed: 7588386]
29. Stocco DM. StAR protein and the regulation of steroid hormone biosynthesis. *Annu Rev Physiol.* 2001; 63:193–213. [PubMed: 11181954]
30. Bhosale P, Bernstein PS. Synergistic effects of zeaxanthin and its binding protein in the prevention of lipid membrane oxidation. *Biochim Biophys Acta.* 2005; 30:116–121. [PubMed: 15949677]
31. Trieschmann M, Beatty S, Nolan JM, Hense HW, Heimes B, Austermann U, Fobker M, Pauleikhoff D. Changes in macular pigment optical density and serum concentrations of its constituent carotenoids following supplemental lutein and zeaxanthin: the LUNA study. *Exp Eye Res.* 2007; 84:718–728. [PubMed: 17306793]
32. Issa PC, van der Veen RL, Stijfs A, Holz FG, Scholl HP, Berendschot TT. Quantification of reduced macular pigment optical density in the central retina in macular telangiectasia type 2. *Exp Eye Res.* 2009; 89:25–31. [PubMed: 19233170]
33. Bernstein PS, Zhao DY, Wintch SW, Ermakov IV, McClane RW, Gellermann W. Resonance Raman measurement of macular carotenoids in normal subjects and in age-related macular degeneration patients. *Ophthalmology.* 2002; 109:1780–1787. [PubMed: 12359594]
34. Nolan JM, Stack J, O'Donovan O, Loane E, Beatty S. Risk factors for age-related maculopathy are associated with a relative lack of macular pigment. *Exp Eye Res.* 2007; 84:61–74. [PubMed: 17083932]
35. Sakudoh T, Iizuka T, Narukawa J, Sezutsu H, Kobayashi I, Kuwazaki S, Banno Y, Kitamura A, Sugiyama H, Takada N, Fujimoto H, Kadono-Okuda K, Mita K, Tamura T, Yamamoto K, Tsuchida K. A CD36-related transmembrane protein is coordinated with an intracellular lipid-binding protein in selective carotenoid transport for cocoon coloration. *J Biol Chem.* 2010; 285:7739–7751. [PubMed: 20053988]

36. During A, Doraiswamy S, Harrison EH. Xanthophylls are preferentially taken up compared with beta-carotene by retinal cells via a SRBI-dependent mechanism. *J Lipid Res.* 2008; 49:1715–1724. [PubMed: 18424859]
37. Kiefer C, Sumser E, Wernet MF, Lintig JV. A class B scavenger receptor mediates the cellular uptake of carotenoids in *Drosophila*. *Proc Natl Acad Sci, U S A.* 2002; 99:10581–10586. [PubMed: 12136129]
38. Tserentsoodol N, Gordiyenko NV, Pascual I, Lee JW, Fliesler SJ, Rodriguez IR. Intraretinal lipid transport is dependent on high density lipoprotein-like particles and class B scavenger receptors. *Mol Vis.* 2006; 12:1319–1333. [PubMed: 17110915]

## ABBREVIATIONS

<b>AMD</b>	age-related macular degeneration
<b>CBP</b>	silkworm lutein-binding protein
<b>CD36</b>	cluster of differentiation 36
<b>GSTP1</b>	glutathione S-transferase pi isoform
<b>HSA</b>	human serum albumin
<b><math>K_D</math></b>	equilibrium dissociation constant
<b>PBT</b>	phosphate buffer containing Triton X-100
<b>RPE</b>	retinal pigment epithelium
<b>SCARB1</b>	scavenger receptor class B, member 1
<b>SPR</b>	surface plasmon resonance
<b>StARD</b>	steroidogenic acute regulatory domain

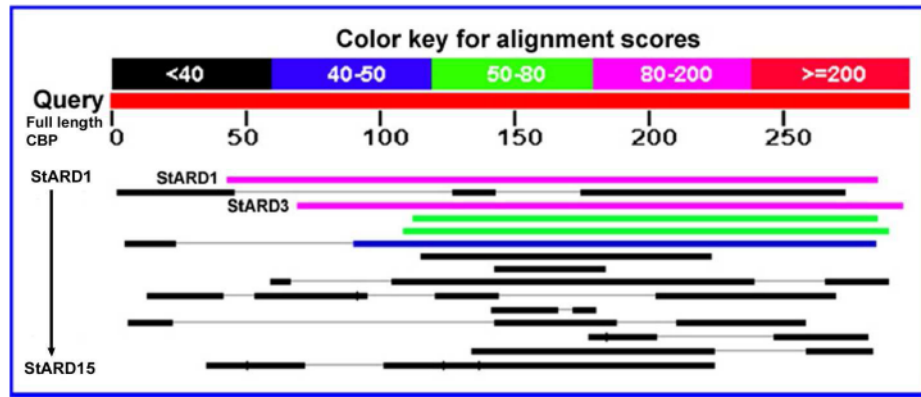


**Figure 1. Alignment results of CBP with all fifteen human StARD sequences**  
 The query sequence is full length CBP from silkworm (*Bombyx mori*). StARD1 and StARD3 show highest similarity to CBP. Their identities to CBP are 25% and 29%, respectively.

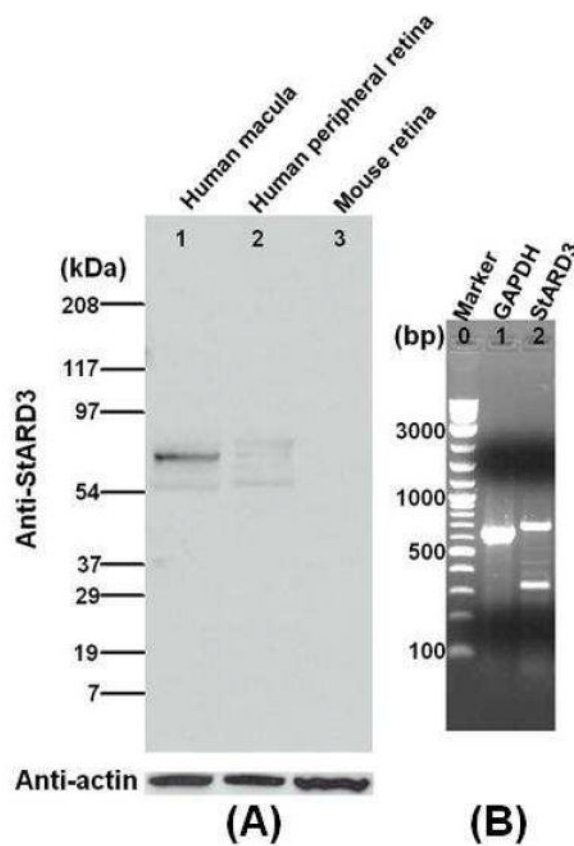


**Figure 2. Western blots of StARD3 antibody against whole protein extracts from retina (A) and RT-PCR of StARD3 from human retina (B)**  
 Western blot lanes: Lane 1, Human macula; Lane 2, Human peripheral retina; Lane 3, Mouse retina. These whole protein extracts were normalized against actin. RT-PCR lanes: Lane 1, Marker; Lane 2, Human GAPDH; Lane 3, StARD3. The upper band of Lane 3 (728 bp) is the correctly-amplified product confirmed by direct sequencing.

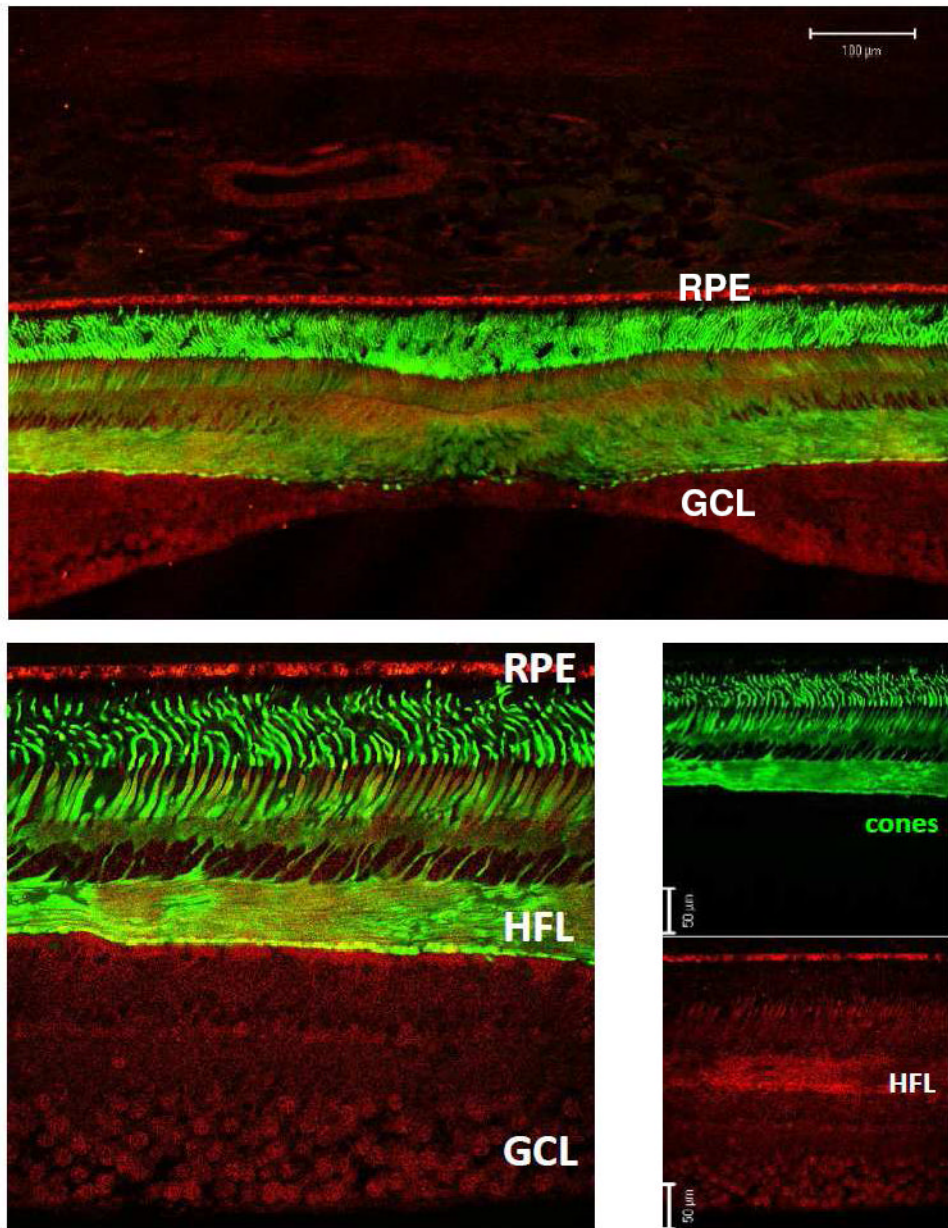


**Figure 3. Low- and high-magnification views of N-62 StAR (red) versus 7G6 (green) immunoreactivity of *Macaca mulatta* parafovea**

Top panel shows a low-magnification view of a near-foveal retina section in which anti-cone arrestin monoclonal antibody (7G6) identifies monkey cones. High-magnification view was imaged temporal from the fovea at 5° eccentricity (lower left). Individual channels (lower right panels) reveal that N-62 StAR antibody labels all neurons of macular retina, and is particularly strong over the Henle fiber layer (HFL) consisting of photoreceptor axons. Abbreviations : RPE, retinal pigment epithelium; GCL, ganglion cell layer. Magnification bars: 100 µm (top panel), 50 µm (lower right).

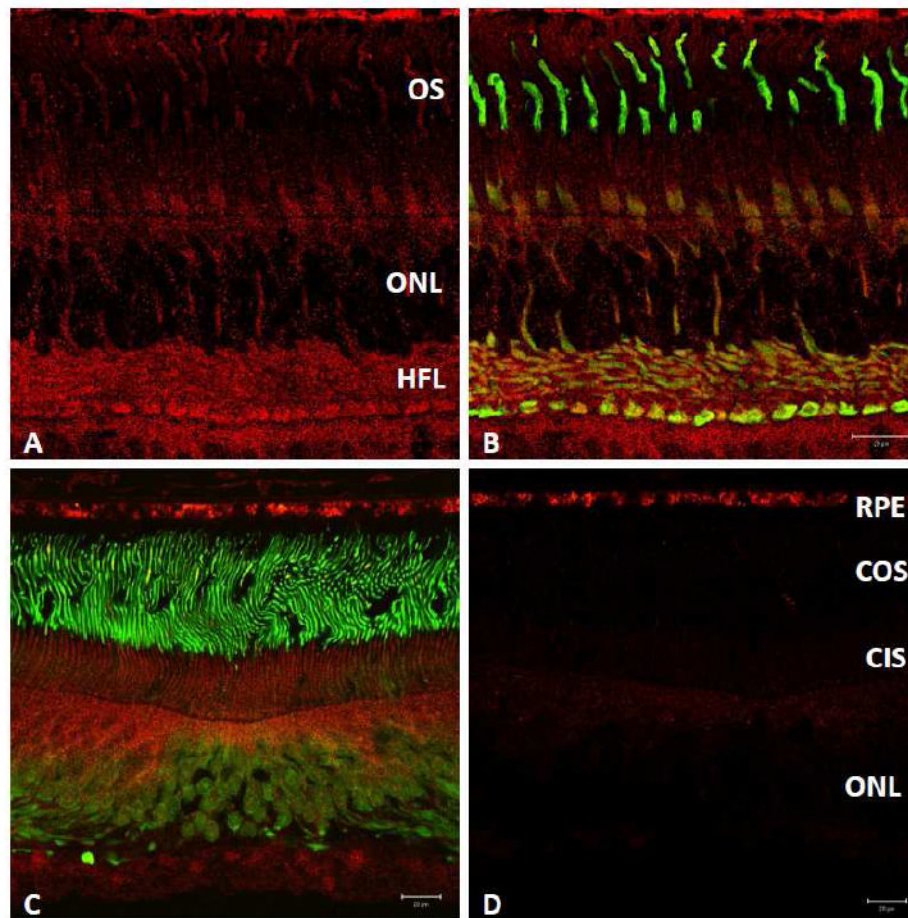


**Figure 4. N-62 StAR (red) immunolabeling of monkey parafoveal cones contrasted with that of cone arrestin (green)**

N-62 StAR antibody labels cone photoreceptors with greater intensity than rods (A, B) within 4-mm temporal from the fovea. Labeled central fovea (C) and preabsorption of N-62 StAR primary antibody with StARD3 protein performed on adjacent section (2.8  $\mu\text{g}$  in 50  $\mu\text{l}$ , D). Competition with StARD3 (D, red channel) abolished almost all signal attributable to N-62 StAR; RPE signal is nonspecific. Abbreviations: ONL, outer nuclear layer; OS, outer segments; COS, cone outer segments; CIS, cone inner segments. Scale bars: 20  $\mu\text{m}$  (B-D).

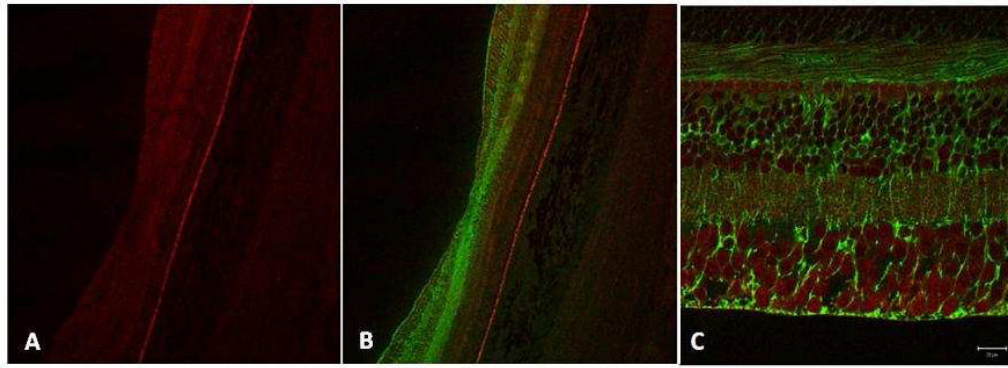


**Figure 5. N-62 StAR (red) versus glutamine synthetase (green) immunolabeling in the monkey parafovea (A-C)**

Antibody directed against StARD3 (N-62 StAR) labels all neurons whereas antibody directed against glutamine synthetase labels Müller cell glia; no colocalization of the two antibodies was observed (C). Magnification bars: 100  $\mu\text{m}$  (A, B), 20  $\mu\text{m}$  (C).



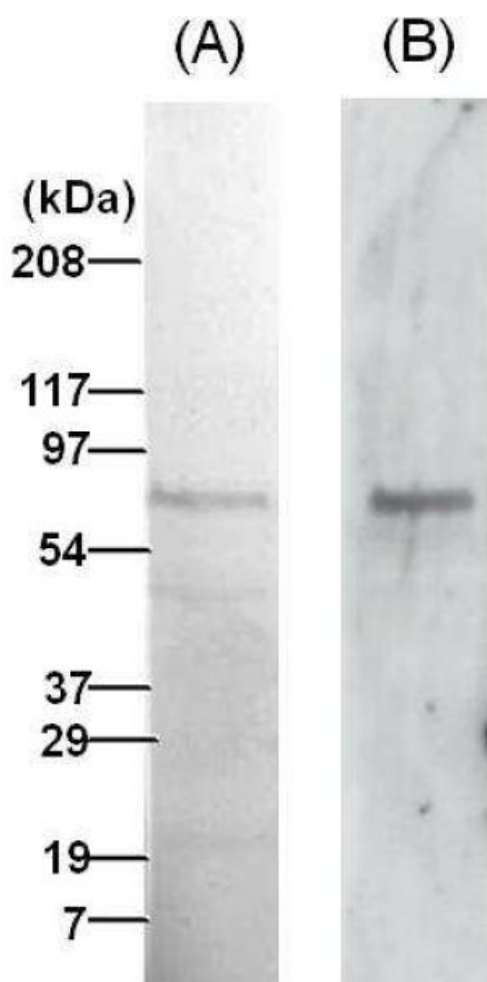


**Figure 6. SDS-PAGE of human recombinant StARD3 (A), and western blot of N-62 StAR antibody against human recombinant StARD3 (B)**

This protein is a StARD3 full-length recombinant protein with a GST tag.

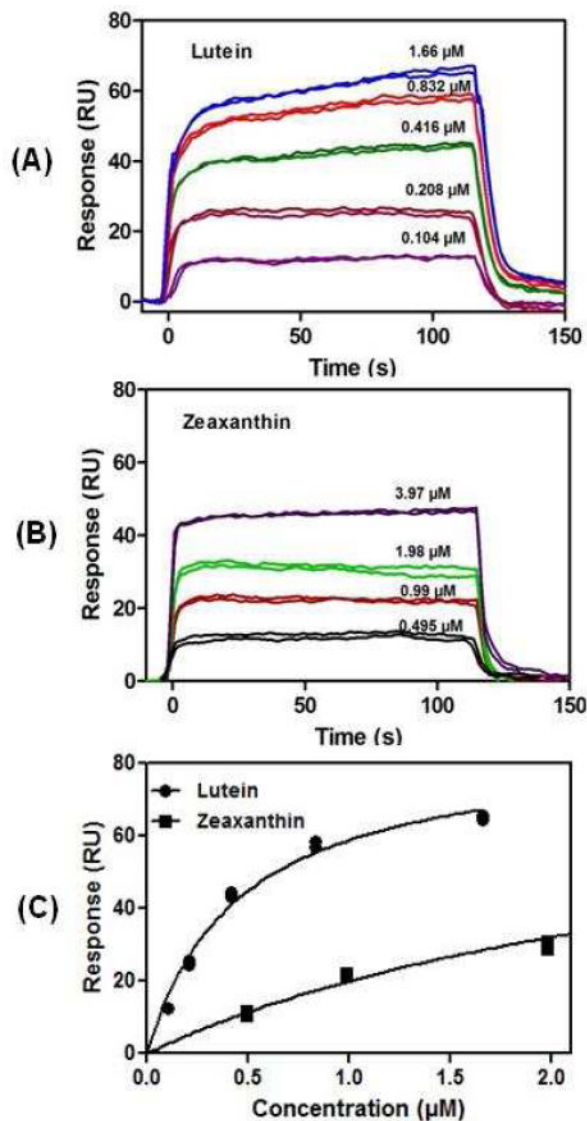


**Figure 7. Surface plasmon resonance (SPR) sensograms of (A) lutein and (B) zeaxanthin binding to immobilized StARD3 protein. (C) Binding isotherm fit of the response shown in (A) and (B)** Responses at equilibrium ( $t = \sim 100\text{-}110$  s) were plotted against injected carotenoid concentrations and fit to a 1:1 binding isotherm. Equilibrium dissociation constants are listed in Table 2.

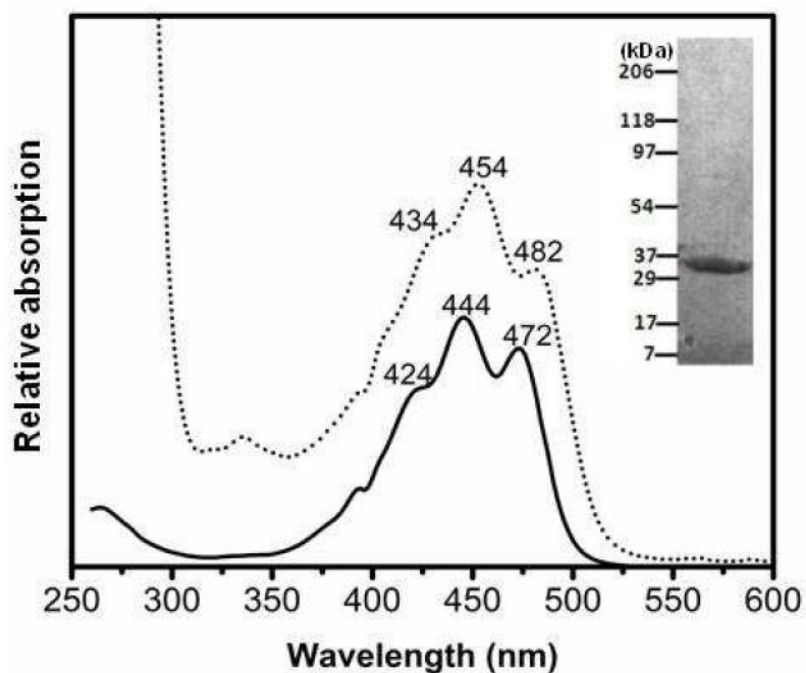


**Figure 8. Absorbance spectra of lutein bound to StARD3 (dotted line, .....)** and lutein in methanol (solid line, —) There is a bathochromic shift of the absorbance peaks of StARD3-lutein complex (434, 454, and 482 nm) relative to unbound lutein (424, 444, and 472 nm). Inset, SDS-PAGE of StARD3 binding domain protein.

Table 1

Western blot results of anti-StARD antibodies against whole protein extracts of human and mouse ocular tissues and livers\*

Antibodies	Total proteins											
	Human macula	Human peripheral retina	Human RPE/choroid	Mouse retina	Mouse RPE/choroid	Human liver	Mouse liver					
StARD1	-	-	-	-	-	-	-	-	-	-	-	-
StARD2	-	-	-	-	-	-	-	-	-	-	-	-
StARD3	+	+/-	+	-	+/-	-	-	-	-	-	-	-
StARD4	-	-	-	-	-	-	-	-	-	-	-	-
StARD5	-	-	-	-	-	-	-	-	-	-	-	-
StARD6	-	-	-	+	+	+	+	+	+	+	+	+
StARD7	-	-	-	-	-	-	-	-	-	-	-	-
StARD8	+	+	+	-	+/-	-	-	-	-	-	-	-
StARD9	-	-	-	-	-	-	-	-	-	-	-	-
StARD10	-	-	-	-	-	+	+	+	+	+	+	+
StARD11	-	-	-	-	-	-	-	-	-	-	-	-
StARD12	-	-	-	-	-	+	+	+	+	+	+	+
StARD13	-	-	-	-	-	-	-	-	-	-	-	-
StARD14	-	-	-	-	-	+	+	+	+	+	+	+
StARD15	-	-	-	-	-	+	+	+	+	+	+	+

\* See Experimental Procedures for detailed information on antibodies and blotting conditions reported in this table. "+," represents a strong band on western blot; "+/-," represents a weak band on western blot; "-" represents no band on western blot.

**Table 2**Equilibrium dissociation constants ( $K_D$ ) determined by surface plasmon resonance (SPR)

Carotenoids	Binding proteins*			
	HSA	CBP	GSTP1	StARD3
Zeaxanthin	1.11 ± 0.03 μM	1.24 ± 0.03 μM	0.09 ± 0.00 μM	2.60 ± 0.10 μM
<i>meso</i> -Zeaxanthin	1.12 ± 0.05 μM	1.14 ± 0.05 μM	0.10 ± 0.01 μM	1.50 ± 0.06 μM
Astaxanthin	1.70 ± 0.30 μM	0.62 ± 0.02 μM	1.30 ± 0.10 μM	1.54 ± 0.02 μM
Lutein	1.69 ± 0.05 μM	0.18 ± 0.01 μM	1.35 ± 0.05 μM	0.45 ± 0.01 μM
β-Carotene	1.20 ± 0.05 μM	0.89 ± 0.02 μM	0.99 ± 0.03 μM	2.09 ± 0.04 μM

\* HSA, human serum albumin; CBP, a lutein-binding protein identified from silkworm; GSTP1, glutathione S-transferase pi isoform (a zeaxanthin-binding protein identified from human retina); StARD3, steroidogenic acute regulatory domain protein, member 3 (a lutein-binding protein identified from human retina). The standard error represents the residual of the model fit. All interactions were consistent with single saturable site interactions with the exception of GSTP1 which had another lower affinity binding site with a  $K_D$  of ~5 μM for each of the tested carotenoids.